Electrogenic Na^+/Ca^{2+} Exchange
A Novel Amplification Step in Squid Olfactory Transduction

Jonathan P. Danaceau*‡ and Mary T. Lucero‡

From the *Interdepartmental Program in Neuroscience, and ‡Department of Physiology University of Utah, School of Medicine, Salt Lake City, Utah 84108

abstract Olfactory receptor neurons (ORNs) from the squid, *Lolliguncula brevis*, respond to the odors l-glutamate or dopamine with increases in internal Ca^{2+} concentrations ($[Ca^{2+}]_i$). To directly asses the effects of increasing $[Ca^{2+}]_i$ in perforated-patched squid ORNs, we applied 10 mM caffeine to release Ca^{2+} from internal stores. We observed an inward current response to caffeine. Monovalent cation replacement of Na^+ from the external bath solution completely and selectively inhibited the caffeine-induced response, and ruled out the possibility of a Ca^{2+}-dependent nonselective cation current. The strict dependence on internal Ca^{2+} and external Na^+ indicated that the inward current was due to an electrogenic Na^+/Ca^{2+} exchanger. Block of the caffeine-induced current by an inhibitor of Na^+/Ca^{2+} exchange (50–100 μM 2′,4′-dichlorobenzamil) and reversibility of the exchanger current, further confirmed its presence. We tested whether Na^+/Ca^{2+} exchange contributed to odor responses by applying the aquatic odor l-glutamate in the presence and absence of 2′,4′-dichlorobenzamil. We found that electrogenic Na^+/Ca^{2+} exchange was responsible for ~26% of the total current associated with glutamate-induced odor responses. Although Na^+/Ca^{2+} exchangers are known to be present in ORNs from numerous species, this is the first work to demonstrate amplifying contributions of the exchanger current to odor transduction.

key words: electrogenic • dichlorobenzamil • chemoreception • sodium–calcium exchange • cephalopod

INTRODUCTION

Calcium plays multiple roles in olfactory transduction. In addition to contributing to the initial transduction current (Firestein and Werblin, 1987; Frings et al., 1995; Leinders-Zufall et al., 1997), increases in intracellular calcium are involved in the amplification of odor-evoked currents in vertebrate olfactory receptor neurons (ORNs)[1] via the activation of calcium-activated chloride currents ($I_{Cl(Ca)}$) (Kleene and Gesteland, 1991; Kurahashi and Yau, 1993; Kleene, 1993, 1997; Lowe and Gold, 1993; Kleene et al., 1994; Kleene and Pun, 1996; Nakamura et al., 1997; Hallani et al., 1998; Reuter et al., 1998). Increases in intracellular calcium have also been implicated in olfactory adaptation, either by increasing phosphodiesterase activity (Borisy et al., 1992), attenuating adenylyl cyclase activity (Wei et al., 1998; Leinders-Zufall et al., 1999), or by decreasing the sensitivity of olfactory cyclic nucleotide–gated channels for cAMP (Kurahashi and Shibuya, 1990; Chen and Yau, 1994; Kurahashi and Menini, 1997; Leinders-Zufall et al., 1998). With so many processes controlled by intracellular calcium, regulating this second messenger is extremely important.

Both Ca^{2+} pumps and Ca^{2+} exchangers are used to regulate intracellular Ca^{2+}. Two classes of electrogenic Ca^{2+} exchangers have been cloned, the Na^+/Ca^{2+}, K^+ exchanger (NCKX) (Cervetto et al., 1989; Reilander et al., 1992) and the Na^+/Ca^{2+} exchanger (NCX); for review, see Blaustein and Lederer (1999). In forward mode, these antiporters exhibit stoichiometries of either 4 Na^+ in 1 Ca^{2+} + 1 K^+ out (NCKX), or 3 Na^+ in 1 Ca^{2+} out (NCX), each resulting in the net inward movement of one positive charge per cycle. The role of NCX has been most extensively documented in cardiac tissue, where it is the predominant method of calcium efflux following contraction, promoting relaxation of myocytes (Hryshko and Philipson, 1997). In addition, NCX appears to be involved in Ca^{2+} entry via reverse Na–Ca exchange during the initial phases of the cardiac action potential, when internal Na^+ is elevated (Hryshko and Philipson, 1997). In mammalian vascular smooth muscle, neurons and astrocytes, the cardiac type NCX appears to be colocalized with underlying endoplasmic or sarcoplasmic reticulum structures, suggesting a role in tightly regulating Ca^{2+} released from intracellular stores (Juhaszova et al., 1996). In cultured retinal amacrine cells, NCX has been shown to be important in terminating synaptic transmission (Gleason et al., 1994). Sodium–calcium exchange has also been well studied in squid axons, where it is involved in regulating intracel-

Address correspondence to Mary T. Lucero, Ph.D., Department of Physiology, University of Utah, 410 Chipeta Way, Room 155, Salt Lake City, UT 84108-1270. Fax: 801-581-3476; E-mail: mary.lucero@m.cc.utah.edu

[1]*Abbreviations used in this paper:* ASW, artificial sea water; DCB - 2′,4′ dichlorobenzamil; ext, external; int, internal; NCKX, Na^+/Ca^{2+}, K^+ exchanger; NCX, sodium calcium exchange; ORN, olfactory receptor neuron.

lular calcium concentrations (DiPolo, 1973, 1977; DiPolo and Beaugé, 1993, 1994a,b). A squid sodium–calcium exchanger, NCX-SQ1, was recently cloned from the stellate ganglia of *Loligo opalescens* (He et al., 1998).

In the olfactory system, sodium–calcium exchange has been localized, both by calcium imaging and immunocytochemistry, to the dendritic knob (and possibly the cilia) of rat ORNs, where it is presumed to clear calcium from the olfactory cilia and dendritic knob after odor stimulation (Noe et al., 1997). In *Xenopus* ORNs, Na^+/Ca^{2+} exchange has been suggested to be present in the dendrites of ORNs (Jung et al., 1994). A more recent study shows that Na^+/Ca^{2+} exchange is required for the termination of $I_{Cl(Ca)}$ (Reisert and Matthews, 1998), and that blocking sodium–calcium exchange prevents recovery from adaptation to odors.

Squid ORNs can be either excited or inhibited by odors (Danaceau and Lucero, 1998, 2000; Lucero et al., 1992), and increases in intracellular calcium have been associated with both types of conductances (Piper and Lucero, 1999; Danaceau and Lucero, 2000). Therefore, we hypothesized that sodium–calcium exchange might be involved in calcium regulation in squid ORNs, following odor responses.

We have used nystatin-perforated patch and whole-cell voltage-clamp recordings to characterize electrogenic sodium–calcium exchange activity in squid ORNs. Forward activity of this exchanger is completely inhibited by removing external Na^+, but is not affected by removal of internal or external K^+. NCX currents are blocked by 2′,4′-dichlorobenzamil (DCB), an inhibitor of sodium–calcium exchange (Frelin et al., 1988). In addition, we show that the NCX current is responsible for ~26% of the current measured after stimulation with glutamate, which activates a mixed cation conductance permeable to calcium > sodium and potassium (Danaceau and Lucero, 2000). This is the first time that an electrogenic sodium–calcium exchanger has been implicated in amplification of olfactory responses in any system.

MATERIALS AND METHODS

Cell Preparation and Culture Conditions

The methods for cell dissociation were similar to those described in Danaceau and Lucero (1998). In brief, the olfactory organs of the squid, *Lolliguncula brevis*, were excised under a dissecting microscope and treated with nonspecific protease (10 mg ml^{-1}, type XIV; Sigma- Aldrich) in sterile filtered artificial sea water (ASW) for 40 min. After a 3–5-min rinse in ASW, the olfactory organ was plated onto a drop of culture medium on concanavalin A (10 mg ml^{-1}, type IV; Sigma-Aldrich)–coated glass coverslips and allowed to settle for 15 min before adding 2 ml medium and placing in the incubator at 17°C. Culture medium was changed daily and the cells were used for experiments between 1 and 3 d in culture. Only the pyriform receptor cell type (Lucero et al., 1992) was used in these experiments.

Solutions

The external bath and internal pipette solutions used in these experiments are listed in Tables I and II. The external and internal solutions were set to an osmolarity of 780 mOsm and a pH of 7.4 or 7.2, respectively. The culture medium consisted of Leibovitz's L-15 (GIBCO BRL) supplemented with salts to bring the osmolarity to 780 mOsm, 2 mM HEPES, pH 7.6, 2 mM l-glutamine, 50 IU ml^{-1} penicillin G, and 0.5 mg ml^{-1} streptomycin. Nystatin stock solution contained 1 mg nystatin / 20 μl DMSO; nystatin internal solution contained 3 μl nystatin stock + 2 μl 10% pluronic acid ml^{-1} internal solution. All internal solutions were kept on ice throughout the experiments.

Chemicals

All chemicals were obtained from Sigma-Aldrich except for DCB, which was obtained from Molecular Probes. DCB was dissolved in DMSO as a 50-mM stock solution before dilution to 50 or 100 μM in ASW.

Nystatin Perforated-Patch Voltage-Clamp Recordings

Nystatin voltage- and current-clamp experiments were essentially similar to those described in Danaceau and Lucero (1998). In brief, 2–5 MΩ resistance electrodes pulled from thick-walled borosilicate filament glass (Sutter Instrument Co.) were filled with nystatin internal solution. Fresh nystatin internal solution was made every 2 h and nystatin stock was remade every 5 h. Gentle suction was applied to form a gigaohm seal. Recordings were made ~5–20 min after seal formation. Bath solutions were perfused through the recording chamber at a rate of 1–2 ml min^{-1}. Test solutions were delivered with an SF-77 rapid solution changer (Warner Instrument Corp.). The application of test solutions was calibrated with an open pipette. There was a delay of ~90 ms between the beginning of the electronic stimulus and the current recorded by the open pipette. We did not correct the data for this delay. A 3-M KCl agar bridge was used to ground the recording chamber.

Whole-Cell Voltage-Clamp Recordings

Whole-cell voltage-clamp recordings were similar to the nystatin patch recordings. The same 2–5-MΩ resistance electrodes were filled with either Na^+-gluconate internal containing Mg^{2+}-ATP or with Li^+-internal solution. The electrode tip was lowered onto the soma of the ORN and gentle suction was applied to form a gigaohm seal. Once the seal was formed, more suction was applied to rupture the membrane patch and achieve whole-cell access. Bath and test solutions were delivered as described for nystatin-perforated patch recordings.

Data Acquisition

Voltage-clamp and current-clamp data were acquired with an Axon Instruments 200A patch clamp amplifier (TL-1-125 Interface; Axon Instruments, Inc.) and a 486, 33 MHz computer using either PClamp 5.6 or Axotape 2.0.2. The data in Figs. 1, 2, and 3 B were sampled at 250 Hz and filtered off line with a digital eight-pole lowpass Bessel filter (Clampfit 8; Axon Instruments, Inc.) using a −3 dB filter cutoff frequency of 35 Hz. The data in Figs. 3 A, 5, and 6 were sampled at 500 Hz and digitally filtered off line with a −3 dB filter cutoff frequency of 50 Hz. The data in Fig. 4 were acquired at 10 kHz and filtered on line with a low pass four-pole Bessel filter cutoff at 5 kHz. Data for capacitance and series resistance (R_s) measurements were sampled at 100 kHz and also filtered on line at 10 kHz (data not shown). The R_s of nystatin-perforated patched cells averaged 39 ± 13 M (SD; n = 18). Ap-

TABLE I

Composition of External Bath Solutions

Bath solution	Na^+	K^+	Ca^{2+}	Mg^{2+}	Li^+	Cl^-	$Tris^+$	Glucose
ASW	344	10	10	35	0	440	0	17.5
Tris ASW	0	0	10	35	0	410	376	10
Li ASW	0	10	10	35	345	445	0	17.5

All solutions contained 10 mM HEPES, were set to pH 7.4 with NaOH or TMAOH and set to an osmolality of 780 mOsm kg^{-1} using d-glucose.

TABLE II

Composition of Internal Pipette Solutions

Internal solution	Na^+	K^+	Cl^-	F^-	$Gluc^-$	TMA^+	TEA^+
Na Gluc with MgATP	328	25	61	25	326	0	52
60 TEA Na Gluc	355	0	61	25	330	0	60
Li Gluc	0	25	61	25	330	0	60
TMA Gluc	25	0	61	25	270	270	60
TMA Cl	25	0	365	25	0	365	0

All solutions were set to pH 7.2 with NaOH or TMAOH and were set to an osmolality of 780 mOsm kg^{-1} with d-glucose. Pipette solutions also contained 0.5 mM Ca^{2+}, 10 mM HEPES, and 1.5 mM EGTA. Nystatin was added to various internal solutions, as described in materials and methods. Gluc, gluconate.

proximately 60–75% of R_s was electrically compensated. The voltage errors associated with the remaining R_s as well as liquid junction potentials were corrected for off line as described in Danaceau and Lucero (1998). All averages are presented as the mean ± SD (n = number of cells).

These experiments comply with NIH publication 86-23, "Principles of Animal Care," revised 1985, and with the current laws of the Unites Stated regarding animal research.

RESULTS

Caffeine Activates a Sodium-dependent Inward Current

Ca^{2+}-imaging experiments have shown that caffeine releases calcium from internal stores in squid ORNs (Piper and Lucero, 1999). When we applied 10 mM caffeine to nystatin-perforated patched squid ORNs, we observed a large inward current (Fig. 1 A). To test whether the caffeine-induced inward current was Na^+ dependent or selective, we substituted either $Tris^+$ or Li^+ for external Na^+. $Tris^+$ is a relatively large organic cation that does not permeate Na^+ channels and should not support either Na^+-selective or -dependent currents. Li^+, on the other hand, is a small, inorganic cation that permeates most Na^+ channels better than Na^+, but cannot replace Na^+ at Na^+-dependent transporters. Li^+ should augment Na^+-selective responses and fail to support Na^+-dependent responses. Replacing external Na^+ with $Tris^+$ completely eliminated the caffeine-induced current (Fig. 1 B). The average magnitude of the caffeine-induced current was −694 ± 349 pA in ASW and −38 ± 23 pA in Tris ASW, a significant 95% reduction (SD; n = 4; paired t test, $P < 0.05$). By dividing the current by the cell capacitance, we obtained the current density under each condition. The current density was 7 ± 4 pA/pF in ASW and 0.4 ± 0.2 pA/pF in $Tris^+$ ASW (Fig. 1 E). In some cells, a small (0.7 ± 0.6 pA/pF; SD; n = 16) chloride-selective component that activated earlier than the large inward current was observed. The early Cl^- current was blocked by 100 μM niflumic acid, reversed at E_{Cl} during ion substitution experiments, and was unaffected by $Tris^+$ substitution (data not shown).

Replacing external Na^+ with Li^+ also eliminated the caffeine-induced inward current (Fig. 1 D). Fig. 1, C and D, shows traces from a single squid ORN treated with 10 mM caffeine in normal ASW and Li^+ ASW, respectively. In this cell, the maximum amplitude of the current was reduced from −807 to −22 pA. In normal ASW, these caffeine-induced currents averaged −788 ± 316 pA (SD; n = 5) and had an average current density of 8 ± 1 pA/pF at −50 mV. However, in Li^+ ASW, the size of the current was significantly reduced by 94% to −44 ± 50 pA and a density of 0.4 ± 0.3 pA/pF (SD; n = 5; paired t test, $P < 0.01$; Fig. 1 E). Inhibition by both $Tris^+$ and Li^+ indicates that the caffeine-induced inward current is Na^+ dependent, as would be expected for forward Na^+/Ca^{2+} exchange rather than a Na^+-selective conductance such as a Ca^{2+}-activated cation channel or a cyclic nucleotide–gated channel. The presence or absence of K^+ in the internal solution did not affect the caffeine-induced current (Fig. 1 A), suggesting that the NCKX is not contributing to the caffeine-induced responses.

DCB Inhibits the Caffeine-activated Current

The dependence of caffeine-activated currents on external Na^+, along with caffeine's ability to liberate internal calcium stores in squid ORNs (Piper and Lucero, 1999), suggested to us that the depolarizing current could be due to an electrogenic sodium–calcium exchanger. To further confirm this hypothesis, we tested the effects of DCB, a blocker of sodium–calcium exchange (Frelin et al., 1988; Kleyman and Cragoe, 1988). Fig. 2 A shows a control response to a 1-s application of 10 mM caffeine in ASW. The two current traces obtained in the presence of DCB are shown in Fig. 2 B. The bath was switched to ASW + 100 μM DCB for 12 s before the first caffeine application in the presence of DCB (Fig. 2 B). The first caffeine + DCB application elicited a reduced current response while the second, which was obtained 30-s later, showed no response. The effect of DCB on this cell was reversible as shown in Fig. 2 C. The caffeine-induced current after DCB wash was 181% of the control; however, the other cells tested either died during DCB washout or did not recover. For the 18 cells treated with caffeine and DCB, the sodium–calcium exchange current was significantly reduced by 95% from an average control current den-

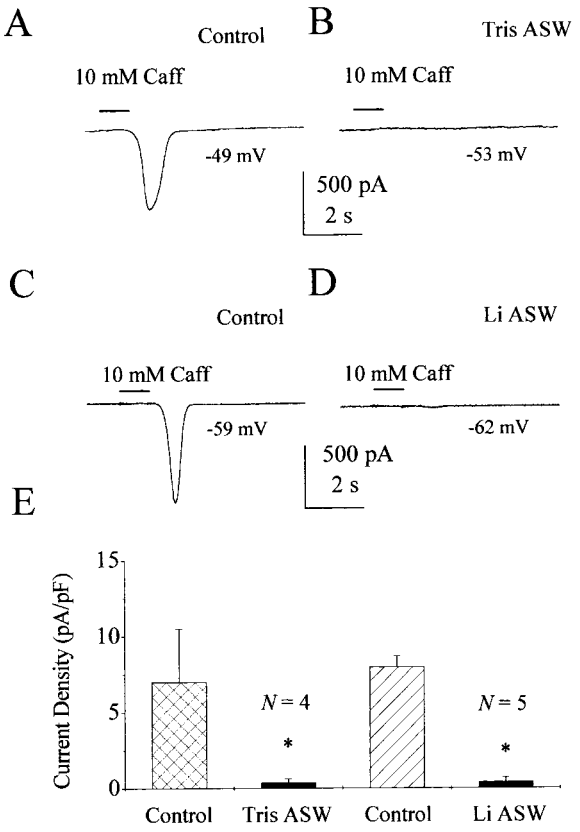

Figure 1. 10 mM caffeine activates a sodium-dependent current in nystatin-perforated patched squid ORNs. (A) Current trace from a nystatin-perforated patched ORN during a 1-s application of 10 mM caffeine. Solutions ASW external (ext)/TMA Cl internal (int). (B) In the same cell, replacing external Na^+ with $Tris^+$ completely eliminated the caffeine-induced current. Solutions: Tris ASW ext/TMA Cl int. (C) A caffeine-activated current response in ASW from a different cell. Same solutions as in A. (D) Current trace from the cell in C in Li^+ ASW. (E) Average current density of caffeine-induced current responses from squid ORNs in ASW, $Tris^+$ ASW, ASW, and Li^+ ASW, respectively. The holding potential has been corrected for liquid junction potential and is indicated in each panel. Error bars indicate SD. $*P < 0.05$.

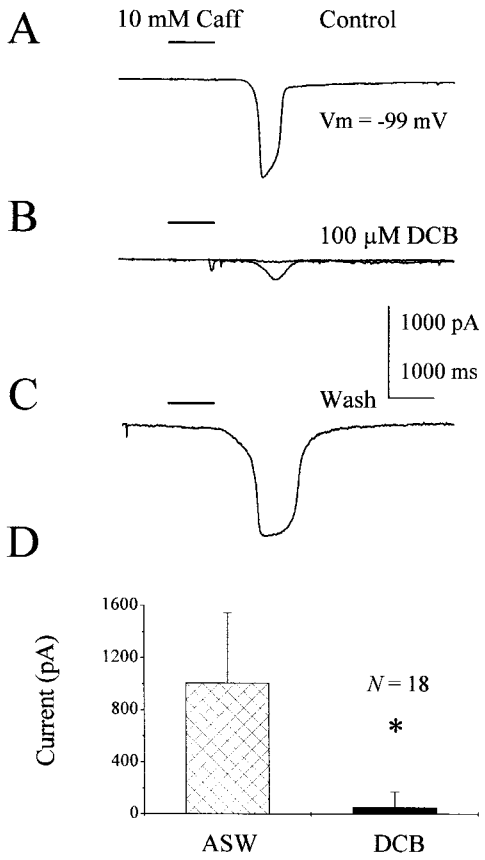

Figure 2. DCB reversibly eliminates Na^+/Ca^{2+} exchange in squid ORNs. (A) 10 mM caffeine elicits a large Na^+/Ca^{2+} exchange current. (B) After 12 s in the presence of 100 μM DCB, I_{NCX} is partially blocked and, after 42 s, I_{NCX} is completely eliminated. (C) After removing DCB and allowing the cell to recover for 2 min, I_{NCX} is restored. (D) In all 18 cells tested, DCB eliminated I_{NCX}. Solutions: ASW ext./Na gluconate int. $*P < 0.001$.

sity of 11 ± 7 to 1 ± 1 pA/pF (SD; $n = 18$; paired t test; $P < 0.001$) (Fig. 2 D). This reduction was statistically significant. The block of the caffeine-induced responses by DCB, along with their elimination in the absence of external Na^+, lead us to conclude that caffeine, by liberating internal calcium stores, activates an electrogenic Na^+/Ca^{2+} exchanger, which generates net inward currents. This caffeine-induced Na^+/Ca^{2+} exchange current will be referred to as I_{NCX}.

Time Course of I_{NCX}

In squid ORNs, odor responses peak within 300–400 ms (Danaceau and Lucero, 2000). The onset of I_{NCX}, however, was delayed relative to odor-induced currents (Fig. 3, A and B). The cell in Fig. 3 illustrates a typical example from a single cell of the delayed onset of the caffeine-induced currents relative to glutamate-induced currents. Note that the caffeine application is over before any NCX current is observed. The time to peak and time to half peak of glutamate-induced responses averaged 382 ± 106 ms (SD; $n = 12$) and 228 ± 64 ms, respectively, at −99 mV. In ASW, the times to peak and half peak of caffeine-induced I_{NCX} averaged 2.0 ± 0.4 and 1.6 ± 0.4 s, respectively, at −88 mV (SD; $n = 9$). We did not correct any data for the ~90-ms delay between the beginning of the trigger of the solution changer and the arrival of test solutions at the cell (see materials and methods). Unlike voltage-gated ion channels, the time to peak for caffeine responses did not change significantly across the voltage range tested (−88 to +52 mV). The marked delay in the onset and time to peak of caffeine responses is presumably due to the time it takes caffeine to diffuse to calcium stores, and for store-released Ca^{2+} to reach high enough concentrations at the cell membrane to activate the exchanger.

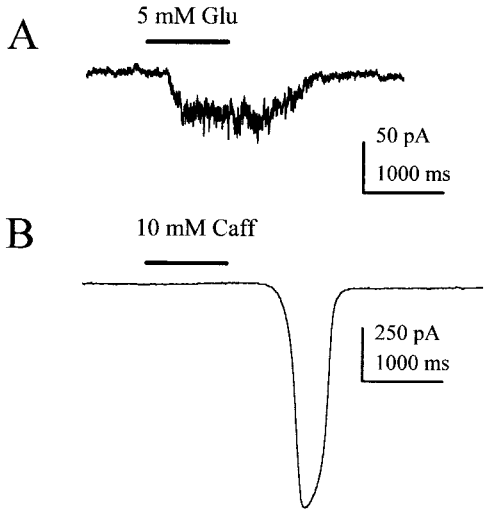

Figure 3. Caffeine-induced currents are delayed relative to odor-induced currents. (A) This current trace was obtained from a nystatin-perforated patched squid ORN during a 1-s application of 5 mM glutamate. (B) In the same cell, the current response to a 1-s application of 10 mM caffeine is markedly delayed. Solutions: ASW ext / TMA gluconate int.

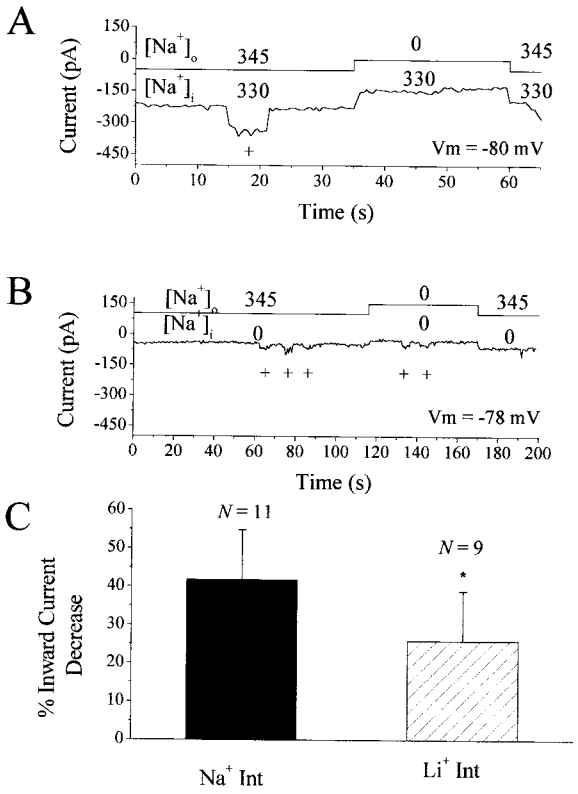

Figure 4. Na^+/Ca^{2+} exchange currents are reversible in squid ORNs. (A) Current traces from a squid ORN under whole-cell voltage-clamp conditions. The solid line above the current trace indicates the switch from ASW to $Tris^+$ ASW. +, 20-mV hyperpolarization. External and internal sodium concentrations are noted above and below the solid line in millimoles per liter^{-1}. Solutions: ASW ext ($Tris^+$ ASW) / Na^+ gluconate int with 4 mM Mg^{2+} and 2 mM ATP. (B) A different ORN exposed to the same protocol as in A, but with Li^+ gluconate internal solution to eliminate reverse Na^+/Ca^{2+} exchange. The solid line indicates the switch from ASW to $Tris^+$ ASW and back again. Numbers indicate external and internal sodium concentrations in millimoles per liter^{-1}. +, 20-mV hyperpolarizations. Solutions: ASW ext ($Tris^+$ ASW) / Li^+ gluconate int; R_s = 19 MΩ, equilibration time = 5 min). (C) Mean percent decrease in the steady state inward current measured during the switch to Tris ASW under the conditions in A (Na^+ int) and B (Li^+ int). *The mean current reduction in Li^+ gluconate is significantly smaller than Na^+ gluconate int $P < 0.05$. Error bars indicate SD; n = numbers of cells.

I_{NCX} Is Reversible

Some Na^+/Ca^{2+} exchangers are capable of acting in either forward or reverse mode (DiPolo, 1989). In forward mode, three Na^+ ions are exchanged for one Ca^{2+} ion, resulting in a net inward flow of current. In reverse mode, the stoichiometry remains the same, but the directions of transport and current flow are reversed. To characterize the reverse mode of Na^+/Ca^{2+} exchange in squid ORNs, we combined whole-cell recording techniques with a high sodium internal solution that also included 4 mM Mg^{2+} and 2 mM ATP to counteract Na^+-dependent inactivation of the exchanger (Collins et al., 1992). After achieving whole-cell access (R_s = 42 ± 12 MΩ, SD; n = 11), the intracellular and pipette solutions were allowed to equilibrate for 13.5 ± 7.6 min before the external bath solution was switched from ASW to $Tris^+$ ASW. The combination of high internal sodium, low internal calcium, zero external sodium, and 10 mM external calcium was expected to stimulate reverse Na^+/Ca^{2+} exchange, resulting in extrusion of Na^+, uptake of Ca^{2+}, and an outward exchanger current. Under these conditions, the removal of external sodium stimulated outward currents (seen as a reduction in the steady state inward leak current) that we attribute to reverse Na^+/Ca^{2+} exchange (Fig. 4 A). As expected, the inward current reduction observed upon removal of external Na^+ was smaller when a Li^+ internal solution was used (Fig. 4 B; R_s = 34 ± 12 MΩ; equilibration time = 3.9 ± 1.9 min; n = 8). To quantify these results, we calculated the percent decrease in the magnitude of the resting inward current obtained when the external bath solution was switched from ASW to $Tris^+$ ASW. With the Li^+ internal solution, the steady state inward current was reduced by 26 ± 13% (SD; n = 9), a significantly smaller decrease than the 42 ± 13% (SD; n = 11) reduction measured with high Na^+ internal solution (Independent Student's t test; $P < 0.05$; Fig. 4 C). Presumably, a longer more complete equilibration of the Li^+ internal would have further reduced the effect on the inward current. Indeed, the cell shown in Fig. 4 B had equilibrated and the switch to $Tris^+$ ASW had very little effect. These results indicate that reverse Na^+/Ca^{2+} exchange can be stimulated by high internal

Na^+ concentrations combined with Na^+ free external solution, and that reverse I_{NCX} can be reduced by replacing internal Na^+ with Li^+.

I_{NCX} Amplifies Odor-induced Currents

To determine if I_{NCX} plays a role in olfactory transduction, we tested its effect on glutamate-activated currents. Glutamate activates a nonselective, calcium-permeable conductance in squid ORNs (Danaceau and Lucero, 2000), and increases in $[Ca^{2+}]_i$ during glutamate responses might be sufficient to activate forward exchange. Fig. 5 A shows current responses of a single ORN treated with glutamate in the presence and absence of 50 μM DCB. In the presence of DCB, the size of the glutamate response in this cell was reduced by 44% from −149 to −83 pA. In the 18 cells tested, the size of the glutamate-induced current was reduced by 26 ± 10% (n = 18), a statistically significant decrease from control conditions (paired t test; $P < 0.05$; Fig. 5 B). We were able to obtain recovery (93 ± 10%) of the original glutamate-induced current in all nine cells that survived long enough for a second control application of glutamate. There was no significant difference between the first and second control glutamate-induced currents (paired t test; $P > 0.05$) confirming that the current reduction seen in the presence of DCB was not due to rundown. The averaged data in Fig. 5 B includes experiments where DCB was preapplied for 1 min (n = 10) and experiments where DCB was coapplied with glutamate (n = 8). There was no difference between data obtained under the two conditions, confirming that the brief preapplication of DCB was not elevating intracellular Ca^{2+}, which could mediate the subsequent reduction in the glutamate response.

Although 2′4′DCB has been established as an inhibitor of Na^+/Ca^{2+} exchange, a closely related compound, 3′4′DCB can inhibit cyclic nucleotide–gated channels (Gomez and Nasi, 1997). We were concerned that the current reductions shown in Fig. 5 could be resulting from a simple block of the glutamate-activated currents by 2′4′DCB. To eliminate this possibility, we compared glutamate responses in ASW and DCB to those in Li^+ ASW. Fig. 5 B shows the average relative glutamate-induced currents in the presence of 50 μM DCB (DCB + Glu) and in the absence of external Na^+ (Li^++ Glu). In both conditions, we eliminated NCX and reduced the total glutamate-induced current by similar amounts. In Li^+ ASW, the glutamate-induced current was reduced by 31 ± 7% (n = 5), a statistically significant decrease from control conditions (paired t test; $P < 0.05$), but not different from the 26 ± 10% reduction observed with DCB (independent t test, $P > 0.05$). The similarity in current reduction when using either Na-free ASW or DCB suggests that DCB is inhibiting I_{NCX} rather than blocking a channel.

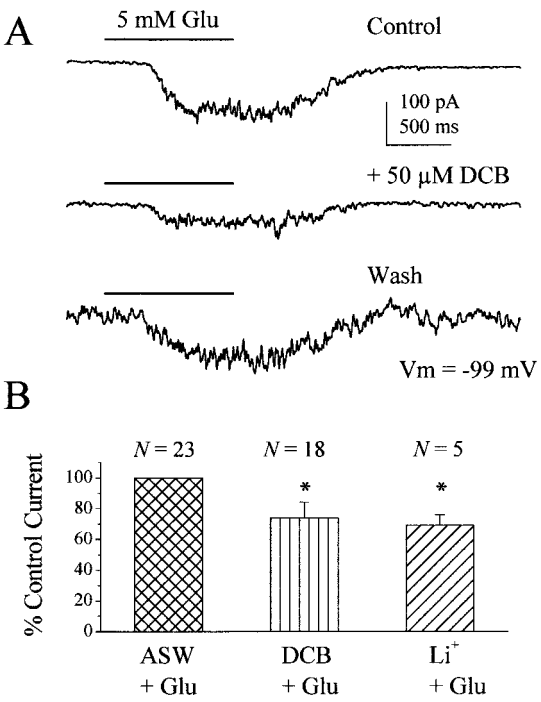

Figure 5. I_{NCX} amplifies odorant responses in squid ORNs. (A) Three successive responses to 5 mM glutamate, 5 mM glutamate in 50 μM DCB, and 5 mM glutamate, respectively, are shown for a nystatin-perforated patched squid ORN. This cell was exposed to DCB for 36 s before application of glutamate + DCB. When DCB is removed, the size of the glutamate-induced current returns to control levels. (B) The magnitude of the peak current was normalized to the peak of the control responses and plotted as a bar graph. DCB was either coapplied with glutamate (n = 8) or preincubated for 58 ± 21 s (n = 10). The combined DCB data show that the response to 5 mM glutamate is reduced by 26 ± 10% (n = 18; vertical stripes). In the absence of external Na^+ (Li^+ + Glu, diagonal stripes), 5 mM glutamate responses were reduced by 31 ± 7%. Error bars indicate SD. *$P < 0.05$. Solutions: ASW ext/60 TEA Na gluconate int.

To further confirm the specificity of DCB, we applied it during glutamate responses in Li^+ ASW. Under these conditions, there should be no Na^+/Ca^{2+} exchange because of the lack of external sodium. Thus, any reduction of the glutamate-activated currents would be due solely to block by DCB. Fig. 6, A and B, shows glutamate-induced current traces from a single squid ORN in Li^+ ASW in the absence and presence of DCB, respectively, and show that DCB has no effect on the size of glutamate-activated currents. The current responses from six cells were normalized to the response to glutamate alone and plotted in Fig. 6 C. In Li^+ ASW, the magnitude of the responses to glutamate in the presence of DCB was 98 ± 14% of the responses to glutamate, a difference that was not significant at the $P > 0.05$ level. These results confirm that Na^+/Ca^{2+} exchange acts to augment or amplify odor responses to glutamate in squid ORNs.

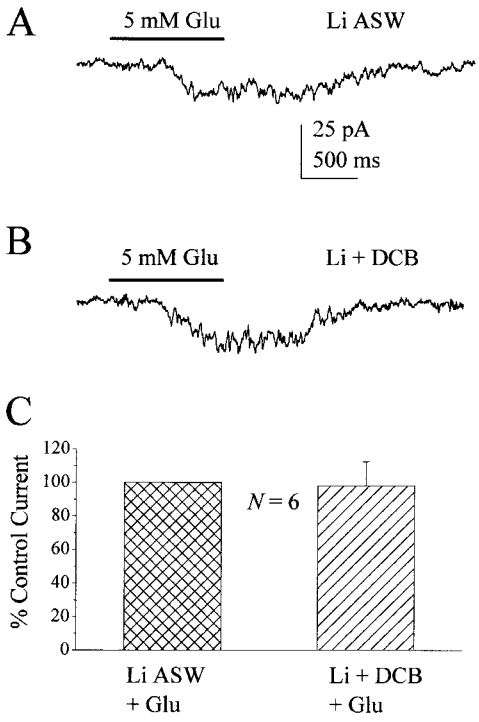

Figure 6. DCB has no effect on glutamate-induced currents in Li^+ ASW. (A) Current trace from a nystatin-perforated patched squid ORN treated with 5 mmol liter^{-1} glutamate in Li^+ ASW. (B) Current trace from the same cell in the presence of 50 μM DCB. Note that the magnitude of the current is unchanged. (C) Bar graph comparing the average, normalized current responses to glutamate from squid ORNs in Li^+ ASW (crosshatch) and in Li^+ ASW + 50 μM DCB (diagonal stripes). In the presence of DCB, responses to glutamate were 98 ± 14% of the control glutamate responses in Li^+ ASW, and were not significantly different from each other ($P > 0.05$). Error bar indicates SD. Solutions: Li^+ ASW ext/60 TEA Na^+ gluconate int.

DISCUSSION

I_{NCX} Is Present in Squid ORNs

We have identified a sodium–calcium exchanger in squid ORNs that is activated by increases in intracellular calcium, dependent upon external sodium, inhibited by DCB, a blocker of sodium–calcium exchange, and which amplifies glutamate-induced inward currents. There was a significant delay in the onset of I_{NCX} activated by caffeine compared with odor responses. The sequential steps required for caffeine-induced I_{NCX} responses could cause this delay. First, caffeine must reach the cell and diffuse through the plasma membrane and the cytosol to reach intracellular Ca^{2+} stores. Then caffeine binds and activates ryanodine receptors that are presumably present and responsible for liberating calcium stores. Finally, the released calcium must diffuse through the cytosol to activate the sodium–calcium exchanger proteins. These steps are contrasted with odor transduction, where, presumably, all of the transduction machinery is located in very close proximity, minimizing diffusion times and resulting in faster kinetics. With regard to the amplification of glutamate responses by I_{NCX}, there was no delay seen for the portion of the current attributed to NCX. The glutamate-induced current and I_{NCX} were concurrent (see Fig. 5). These results suggest that some NCX proteins are located in very close proximity to the transduction channels for glutamate-induced odor responses, and that the delay between caffeine application and I_{NCX} is due to the several diffusion and binding steps mentioned above and not to any property of the sodium–calcium exchanger itself. In support of this hypothesis, our recent immunological study using a polyclonal antibody against the cloned squid NCX (NCX-SQ1) showed specific staining localized to the cilia of the pyriform cell type used in the present studies (Lucero et al., 2000).

Ionic Dependence of I_{NCX}

We have shown that forward Na^+/Ca^{2+} exchange in squid ORNs is blocked by the replacement of external Na^+ with either $Tris^+$ or Li^+. In addition, there does not appear to be any dependence upon internal K^+. In all of the experiments except for those presented in Fig. 4, there was no K^+ present in the internal pipette solutions. These ionic requirements are consistent with the NCX type Na^+/Ca^{2+} exchangers, including the mammalian cardiac exchanger, NCX1, and the recently cloned NCX-SQ1 from squid (He et al., 1998; Hryshko and Philipson, 1997). Furthermore, the lack of a requirement for internal K^+ argues that this exchanger is not related to the Na^+/Ca^{2+}, K^+ exchanger from rod photoreceptors (Cervetto et al., 1989; Reilander et al., 1992). Thus, squid ORNs possess a classical NCX-type Na^+/Ca^{2+} exchanger.

Reversal of I_{NCX}

In addition to forward Na^+/Ca^{2+} exchange stimulated by caffeine application, we have also demonstrated reverse Na^+/Ca^{2+} exchange in squid ORNs. This, again, is consistent with results seen for other NCX-type exchangers and with the squid Na^+/Ca^{2+} exchanger, NCX-SQ1 (He et al., 1998). Upon removal of external sodium, we observed a decrease in the inward holding current of squid ORNs in the presence of a high Na^+ internal solution containing Mg^{2+} and ATP. We attribute the reduction in recorded inward current to the generation of a net outward current during reverse NCX. Under conditions that should have eliminated reverse NCX (Li^+ internal solutions), the removal of external Na^+ resulted in a significantly smaller reduction in the holding current compared with the Na^+ internal solution. Incomplete dialysis of the Li^+ internal solution may account for the residual reverse NCX observed. The difference in current reduction between the two internal condi-

tions reflects the relative amount of reverse Na^+/Ca^{2+} exchange generated by increasing internal Na^+.

Amplification of Odor Responses

Olfactory receptor potentials in several species have been shown to consist of at least two current responses, an initial transduction current, followed by (or coupled with) an amplification current. In vertebrate ORNs, calcium-activated chloride currents amplify the initial transduction current (Kleene and Gesteland, 1991; Kleene, 1993; Kurahashi and Yau, 1993; Lowe and Gold, 1993; Kleene and Pun, 1996; Kleene, 1997; Nakamura et al., 1997; Reuter et al., 1998). Amplification of olfactory signals has been reported in invertebrates as well. In lobster, initial odor-activated conductances that are permeable to sodium and calcium (Fadool and Ache, 1992) are amplified by sodium-activated cation channels (Zhainazarov and Ache, 1997; Zhainazarov et al., 1998). In addition, a calcium-activated cation channel has been described in ORNs from the moth *Manduca sexta* that may be involved in augmenting the initial depolarizing odor response (Zufall et al., 1991). To our knowledge, this is the first report of direct amplification of an odor response by an electrogenic ion exchanger.

The reduction in the glutamate-induced current in the presence of Li^+ or DCB was not due to a buildup of intracellular Ca^{2+} acting directly on the transduction machinery because coapplication of glutamate and DCB produced the same inhibition as a 1 min preincubation in DCB. In addition, we showed that in the absence of NCX, DCB had no effect on the glutamate-induced current (Fig. 6). Thus, the component of glutamate-induced current inhibited by DCB or Li^+ application appears to be I_{NCX} and not an indirect effect of the experimental conditions.

In frog, sodium–calcium exchange appears to be involved in terminating olfactory responses. By removing $[Ca]_i$, the size and duration of $I_{Cl(Ca)}$ is reduced. Conversely, the duration of $I_{Cl(Ca)}$ is prolonged when sodium–calcium exchange is blocked by eliminating external Na^+ (Reisert and Matthews, 1998). In the present study, we see an opposite role for sodium–calcium exchange. Instead of contributing towards adaptation, the squid sodium–calcium exchanger is involved in amplifying odor responses. Furthermore, we show that this amplification is due to the electrogenic properties of the exchanger itself, as opposed to *Rana*, where only the effects of removing $[Ca^{2+}]_i$ were reported (Reisert and Matthews, 1998).

Use of NCX during glutamate responses in squid ORNS results in a 1.5× amplification of the original Ca^{2+} signal. This observation can be verified algebraically. We start with the simple equation:

$$IGlu_{total} = IGlu_{Ca}{}^{2+} + IGlu^{+} + I_{NCX}Ca_{influx}, \quad (1)$$

where $IGlu_{total}$ = the total current recorded during glutamate application, $IGlu_{Ca}{}^{2+}$ is the glutamate-induced current carried by Ca^{2+} influx through the transduction channel, $IGlu^+$ is the glutamate-induced current carried by monovalent cations through the transduction channel, and $I_{NCX}Ca_{influx}$ is the net inward current of the exchanger activated by Ca^{2+} influx. If we take the extreme case where Ca^{2+} carries all of the current that enters the transduction channel during a glutamate response, then $IGlu^+$ reduces to zero and Eq. 1 becomes:

$$IGlu_{total} = IGlu_{Ca}{}^{2+} + I_{NCX}Ca_{influx}. \quad (2)$$

For every 2+ charges that enter the cell as Ca^{2+}, 3+ charges enter as Na^+ on NCX, resulting in a 1.5× amplification of the Ca^{2+} signal. Assuming that the only Ca^{2+} available to the exchanger is via influx, then

$$IGlu_{Ca}{}^{2+} = 2 \cdot I_{NCX}Ca_{influx}. \quad (3)$$

Since under the hypothetical conditions of a Ca^{2+}-selective transduction channel, two thirds of $IGlu_{total}$ is carried by Ca^{2+}, we can substitute % values into Eq. 2, where (Eq. 4):

$$100\% = 66.7\% + 33.3\%. \quad (4)$$

This means that if all of the current through the transduction channel were carried by Ca^{2+}, then total block of I_{NCX} would reduce $IGlu_{total}$ by 33.3%. If reduction of $IGlu_{total}$ was <33.3% then, by substituting Eq. 3 into 1 and rearranging we see that the contribution of monovalent cations ($IGlu^+$) to the total glutamate-induced current is (Eq. 5):

$$IGlu^{+} = IGlu_{total} - (3 \cdot I_{NCX}). \quad (5)$$

If block of I_{NCX} reduces $IGlu_{total}$ by >33.3%, then, in addition to Ca^{2+} influx, Ca^{2+} released from intracellular stores must contribute to I_{NCX} ($I_{NCX}Ca_{stores}$) and the total I_{NCX} ($I_{NCXtotal}$) becomes (Eq. 6):

$$I_{NCXtotal} = IGlu_{total} - IGlu_{Ca}{}^{2+} + I_{NCX}Ca_{stores}. \quad (6)$$

Rearranging and including contributions from monovalent cations gives the final form of the equation describing the glutamate-induced current (Eq. 7):

$$IGlu_{total} = IGlu_{Ca}{}^{2+} + IGlu^{+} + I_{NCXtotal}. \quad (7)$$

We showed that regardless of whether I_{NCX} was blocked by DCB or not supported by Li^+ replacement of external Na^+, $IGlu_{total}$ was reduced on average by 26–31%. These findings indicate that the majority (70% or more) of the current through the glutamate-induced

transduction channel is carried by Ca^{2+}, and that there is a small contribution (22% or less) by monovalent cations. If we look at individual cells, we see that in some cells, $I_{NCX\ total}$ contributes >40% of the current. In these cases, we suggest that Ca^{2+} released from intracellular stores is contributing to the total Ca^{2+} available to the exchanger and further amplifying the current. In general, the contribution of Ca^{2+} by store release was modest and only observed in a subset of cells (4/18 cells in DCB, 2/5 cells in Li^+). Thus, activation of NCX during glutamate responses appears to be mainly dependent on Ca^{2+} influx through a glutamate-activated transduction channel ($IGlu_{Ca}{}^{2+}$). These observations correlate well with our earlier studies showing that the glutamate-induced current in squid ORNs has a much higher selectivity for Ca^{2+} over Na^+ or K^+ (Danaceau and Lucero, 2000). We do not know yet whether the glutamate-induced transduction channel is an integral part of the glutamate receptor (ionotropic receptor) or a cyclic nucleotide–gated channel; however, we do see similar currents with internal perfusion of cAMP (Lucero and Piper, 1994).

In addition to depolarizing odor responses, squid ORNs respond to some odors (all aversive so far) with hyperpolarizing responses (Lucero et al., 1992; Danaceau and Lucero, 1998). One hyperpolarizing odor, betaine, activates a chloride conductance that is calcium independent (Danaceau and Lucero, 1998; Piper and Lucero, 1999), while a different odor, dopamine, induced hyperpolarizing responses that are associated with increases in intracellular calcium (Piper and Lucero, 1999). The sodium–calcium exchanger described in this paper could contribute to olfactory adaptation of a hyperpolarizing, calcium-dependent response in two ways. First, olfactory responses that are dependent upon increases in intracellular calcium would be attenuated as the exchanger cleared intracellular calcium from the cytosol. Second, the depolarizing electrogenic properties of the exchanger would oppose the hyperpolarizing responses elicited by dopamine, counteracting membrane hyperpolarization. Future experiments will be needed to investigate these hypotheses.

We thank J.D. Lucero, T. Dang, and Dr. C. Hegg for technical assistance and the National Resource Center for Cephalopods (Galveston, TX) for providing squids. We also thank Drs. W.C. Michel, H.M. Brown, D. Piper, and K. Spitzer for helpful comments on the manuscript.

This work was supported by National Institutes of Health (NIH) National Institute on Deafness and Other Communication Disorders grant DC02587 to M.T. Lucero.

Submitted: 25 October 1999
Revised: 25 April 2000
Accepted: 27 April 2000

REFERENCES

Blaustein, M.P., and W.J. Lederer. 1999. Sodium/calcium exchange: its physiological implications. *Physiol. Rev.* 79:763–854.

Borisy, F.F., G.V. Ronnett, A.M. Cunningham, D. Juilfs, J. Beavo, and S.H. Snyder. 1992. Calcium/calmodulin-activated phosphodiesterase expressed in olfactory receptor neurons. *J. Neurosci.* 12: 915–923.

Cervetto, L., L. Lagnado, R.J. Perry, D.W. Robinson, and P.A. McNaughton. 1989. Extrusion of calcium from rod outer segments is driven by both sodium and potassium gradients. *Nature.* 337: 740–743.

Chen, T.-Y., and K.-W. Yau. 1994. Direct modulation by Ca^{2+}-calmodulin of cyclic nucleotide-activated channel of rat olfactory receptor neurons. *Nature.* 368:545–548.

Collins, A., A.V. Somlyo, and D.W. Hilgemann. 1992. The giant cardiac membrane patch method: stimulation of outward Na–Ca exchange current by MgATP. *J. Physiol.* 454:27–57.

Danaceau, J.P., and M.T. Lucero. 1998. Betaine activates a hyperpolarizing chloride conductance in squid olfactory receptor neurons. *J. Comp. Physiol. A Sens. Neural Behav. Physiol.* 183:225–235.

Danaceau, J.P., and M.T. Lucero. 2000. Mixture interactions of glutamate and betaine in single squid olfactory neurons. *J. Comp. Physiol. A Sens. Neural Behav. Physiol.* 186:57–67.

DiPolo, R. 1973. Calcium efflux from internally dialyzed squid giant axons. *J. Gen. Physiol.* 62:575–589.

DiPolo, R. 1977. Characterization of the ATP-dependent calcium efflux in dialyzed squid giant axons. *J. Gen. Physiol.* 69:795–813.

DiPolo, R. 1989. The sodium–calcium exchange in intact cells. *In* Sodium–Calcium Exchange. T.J.A. Allen, D. Noble, and H. Reuter, editors. Oxford University Press, New York, NY. 5–26.

DiPolo, R., and L. Beaugé. 1993. Effects of some metal-ATP complexes on Na^+–Ca^{2+} exchange in internally dialyzed squid axons. *J. Physiol.* 462:71–86.

DiPolo, R., and L. Beaugé. 1994a. Cardiac sarcolemmal Na/Ca-inhibiting peptides XIP and FMRF-amide also inhibit Na/Ca exchange in squid axons. *Am. J. Physiol. Cell Physiol.* 363:C307–C311.

DiPolo, R., and L. Beaugé. 1994b. Effects of vanadate on MgATP stimulation of Na/Ca exchange support kinase-phosphatase modulation in squid axons. *Am. J. Physiol. Cell Physiol.* 363:C1382–C1391.

Fadool, D.A., and B.W. Ache. 1992. Plasma membrane inositol 1,4,5-trisphosphate-activated channels mediate signal transduction in lobster olfactory receptor neurons. *Neuron.* 9:907–918.

Firestein, S., and F.S. Werblin. 1987. Gated currents in isolated olfactory receptor neurons of the larval tiger salamander. *Proc. Natl. Acad. Sci. USA.* 84:6292–6296.

Frelin, C., P. Barbry, P. Vigne, O. Chassande, E.J. Cragoe, Jr., and M. Lazdunski. 1988. Amiloride and its analogs as tools to inhibit Na^+ transport via the Na^+ channel, the Na^+/H^+ antiport and the Na^+/Ca^{2+} exchanger. *Biochimie.* 70:1285–1290.

Frings, S., R. Seifert, M. Godde, and U.B. Kaupp. 1995. Profoundly different calcium permeation and blockage determine the specific function of distinct cyclic nucleotide–gated channels. *Neuron.* 15:169–179.

Gleason, E., S. Borges, and M. Wilson. 1994. Control of transmitter release from retinal amacrine cells by Ca^{2+} influx and efflux. *Neuron.* 13:1109–1117.

Gomez, M.P., and E. Nasi. 1997. Antagonists of the cGMP-gated conductance of vertebrate rods block the photocurrent in scallop ciliary photoreceptors. *J. Physiol.* 500:367–378.

Hallani, M., J.W. Lynch, and P.H. Barry. 1998. Characterization of calcium-activated chloride channels in patches excised from the dendritic knob of mammalian olfactory receptor neurons. *J. Membr. Biol.* 161:163–171.

He, Z., Q. Tong, B.D. Quednau, K.D. Philipson, and D.W. Hilgemann. 1998. Cloning, expression, and characterization of the squid Na^+–Ca^{2+} exchanger (NCX-SQ1). *J. Gen. Physiol.* 111:857–873.

Hryshko, L.V., and K.D. Philipson. 1997. Sodium-calcium exchange: recent advances. *Basic Res. Cardiol.* 92:45–51.

Juhaszova, M., H. Shimizu, M. Borin, R.K. Yip, E.M. Santiago, G.E. Lindenmayer, and M.P. Blaustein. 1996. Localization of the Na^+–Ca^{2+} exchanger in vascular smooth muscle, and in neurons and astrocytes. *Ann. NY Acad. Sci.* 779:318–335.

Jung, A., F.W. Lischka, J. Engel, and D. Schild. 1994. Sodium/calcium exchanger in olfactory receptor neurones of *Xenopus laevis*. *Neuroreport.* 5:1741–1744.

Kleene, S.J. 1993. Origin of the chloride current in olfactory transduction. *Neuron*. 11:123–132.

Kleene, S.J. 1997. High-gain, low-noise amplification in olfactory transduction. *Biophys. J.* 73:1110–1117.

Kleene, S.J., and R.C. Gesteland. 1991. Calcium-activated chloride conductance in frog olfactory cilia. *J. Neurosci*. 11:3624–3629.

Kleene, S.J., R.C. Gesteland, and S.H. Bryant. 1994. An electrophysiological survey of frog olfactory cilia. *J. Exp. Biol.* 195:307–328.

Kleene, S.J., and R.Y.K. Pun. 1996. Persistence of the olfactory receptor current in a wide variety of extracellular environments. *J. Neurophysiol.* 75:1386–1391.

Kleyman, T.R., and E.J. Cragoe. 1988. Amiloride and its analogs as tools in the study of ion transport. *J. Membr. Biol.* 105:1–21.

Kurahashi, T., and A. Menini. 1997. Mechanism of odorant adaptation in the olfactory receptor cell. *Nature.* 385:725–729.

Kurahashi, T., and T. Shibuya. 1990. Ca^{2+}-dependent adaptive properties in the solitary olfactory receptor cell of the newt. *Brain Res.* 515:261–268.

Kurahashi, T., and K.W. Yau. 1993. Co-existence of cationic and chloride components in odorant-induced current of vertebrate olfactory receptor cells. *Nature.* 363:71–74.

Leinders-Zufall, T., C.A. Greer, G.M. Shepherd, and F. Zufall. 1998. Visualizing odor detection in olfactory cilia by calcium imaging. *Ann. NY Acad. Sci.* 855:205–207.

Leinders-Zufall, T., M. Ma, and F. Zufall. 1999. Impaired odor adaptation in olfactory receptor neurons after inhibition of Ca^{2+}/calmodulin kinase II. *J. Neurosci.* 19:1–6.

Leinders-Zufall, T., M.N. Rand, G.M. Shepherd, C.A. Greer, and F. Zufall. 1997. Calcium entry through cyclic nucleotide–gated channels in individual cilia of olfactory receptor cells: spatiotemporal dynamics. *J. Neurosci.* 17:4136–4148.

Lowe, G., and G.H. Gold. 1993. Nonlinear amplification by calcium-dependent chloride channels in olfactory receptor cells. *Nature.* 366:283–286.

Lucero, M.T., F.T. Horrigan, and W.F. Gilly. 1992. Electrical responses to chemical stimulation of squid olfactory receptor cells. *J. Exp. Biol.* 162:231–249.

Lucero, M.T., and D.R. Piper. 1994. IP_3 and cyclic nucleotides elicit opposite membrane potential changes in squid olfactory receptor neurons. *Chem. Senses.* 19:509. (Abstr.)

Lucero, M.T., W. Huang, and T. Dang. 2000. Immunohistochemical evidence for the Na^+/Ca^{2+} exchanger in squid olfactory neurons. *Philos. Trans. R. Soc. Lond. B Biol. Sci.* In press.

Nakamura, T., N. Nishida, and H. Kaneko. 1997. Direct measurement of concentration of chloride in the newt olfactory cell. *Chem. Senses.* 22:757–758. (Abstr.)

Noe, J., E. Tareilus, I. Boekhoff, and H. Breer. 1997. Sodium/calcium exchanger in rat olfactory neurons. *Neurochem. Int.* 30:523–531.

Piper, D.R., and M.T. Lucero. 1999. Calcium signalling in squid olfactory receptor neurons. *Biol. Signals Recept.* 8:329–337.

Reilander, H., A. Achilles, U. Friedel, G. Maul, F. Lottspeich, and N.J. Cook. 1992. Primary structure and functional expression of the Na/Ca,K exchanger from bovine rod photoreceptors. *EMBO (Eur. Mol. Biol. Organ.) J.* 11:1689–1695.

Reisert, J., and H.R. Matthews. 1998. Na^+-dependent Ca^{2+} extrusion governs response recovery in frog olfactory receptor neurons. *J. Gen. Physiol.* 112:529–535.

Reuter, D., K. Zierold, W.H. Schroder, and S. Frings. 1998. A depolarizing chloride current contributes to chemoelectrical transduction in olfactory sensory neurons in situ. *J. Neurosci.* 18:6623–6630.

Wei, J., A.Z. Zhao, G.C.K. Chan, L.P. Baker, S. Impey, J.A. Beavo, and D.R. Storm. 1998. Phosphorylation and inhibition of olfactory adenylyl cyclase by CaM kinase II in neurons: a mechanism for attenuation of olfactory signals. *Neuron*. 21:495–504.

Zhainazarov, A.B., and B.W. Ache. 1997. Gating and conduction properties of a sodium-activated cation channel from lobster olfactory receptor neurons. *J. Membr. Biol.* 156:173–190.

Zhainazarov, A.B., R.E. Doolin, and B.W. Ache. 1998. Sodium-gated cation channel implicated in the activation of lobster olfactory receptor neurons. *J. Neurophysiol.* 79:1349–1359.

Zufall, F., H. Hatt, and T.A. Keil. 1991. A calcium-activated nonspecific cation channel from olfactory receptor neurones of the silkmoth *Antheraea polyphemus*. *J. Exp. Biol.* 161:455–468.